

## Rational finite element method for plane orthotropic elastic problems

Ling Mao, Weian Yao, Qiang Gao\* and Wanxie Zhong

State Key Laboratory of Structural Analysis for Industrial Equipment, Dalian University of Technology,  
Dalian, 116024, P.R. China

(Received September 3, 2012, Revised April 15, 2014, Accepted May 12, 2014)

**Abstract.** The rational finite element method is different from the standard finite element method, which is constructed using basic solutions of the governing differential equations as interpolation functions in the elements. Therefore, it is superior to the isoparametric approach because of its obvious physical meaning and accuracy; it has successfully been applied to the isotropic elasticity problem. In this paper, the formulation of rational finite elements for plane orthotropic elasticity problems is deduced. This method is formulated directly in the physical domain with full consideration of the requirements of the patch test. Based on the number of element nodes and the interpolation functions, different approaches are applied with complete polynomial interpolation functions. Then, two special stiffness matrixes of elements with four and five nodes are deduced as a representative application. In addition, some typical numerical examples are considered to evaluate the performance of the elements. The numerical results demonstrate that the present method has a high level of accuracy and is an effective technique for solving plane orthotropic elasticity problems.

**Keywords:** orthotropic; elastic problem; rational finite element method

---

### 1. Introduction

In elasticity, the solutions to most problems require numerical methods, except for a few problems with simple loads, regular domains and simple boundary conditions. A significant amount of research was done in the field after the presentation of the finite element method (FEM) (Turener *et al.* 1956). FEM establishes equations using the variation of the energy functional and the interpolation of piecewise polynomials.

The finite element is divided into two components, i.e., a univariate element and a multivariate element, according to the number of field variable. Based on the idea of FEM and different requirements, new methods have been developed, such as the partition of unity finite element method (PUFEM, Melenk and Babuska 1996), the extended finite element method (XFEM, Areias and Belytschko 2005), the generalized finite element method (GFEM, Duarte *et al.* 2000, Simone *et al.* 2006), and the hybrid finite element method (HFEM, Xue 1985). To some extent, these methods are divided between mechanical problems and mathematical problems. For example, for

---

\*Corresponding author, Ph.D., E-mail: [qgao@dlut.edu.cn](mailto:qgao@dlut.edu.cn)

the standard FEM, the isoparametric element technology requires the generated shape function to satisfy the patch test, while for the GFEM, the grid and real physical domain are not the same.

Hybrid-Trefftz element (Jirousek and Venkatesh 1992, Venkatseh and Jirousek 1995) uses Trefftz complete solution as the element interpolation function. Zhong and Ji (1996) proposed rational FEM (RFEM) in which the interpolation function is the linear combination of analytical solutions of the elastic problem, so the field variables can be formulated directly in the physical domain. This method considered the requirement of the patch test at the element level and adequately used the analytical solution from the mechanics problems (Zhong 1997, Zhong and Ji 1997). Different from standard FEM, all of the solution processes of RFEM are in the physical domain, and the isoparametric transformation is avoided. Ji and Zhong (1997) derived plane RFEM with 4 and 5 nodes using the complete quadratic solution, and then presented a convergence proof for RFEM, which gives a firm theoretical foundation for RFEM. Ji *et al.* (2000) extended RFEM to an 8-node curve quadrilateral, and Wang and Zhong (2002, 2003) provided the formulation for 8-node and 20-node hexahedrons. Long *et al.* (2009) proposed the generalized conforming element method based on analytical trial function. According to the principle of minimum complementary energy, Fu *et al.* (2010) presented a new 8-node plane element ATF-Q8 by taking the Airy stress function. Cen *et al.* (2011) established a plane hybrid stress-function element method for anisotropic materials. Cen *et al.* (2012) proposed a new high precision plane element US-ATFQ8, by introducing the analytical trial function method and the hybrid stress-function element method into the unsymmetrical FEM.

Second only to the isotropic problem, the orthotropic problem is widely researched. In biomechanics (Hambli *et al.* 2012), rock mechanics, fracture mechanics (Bambill *et al.* 2009, Beom *et al.* 2012, Karihaloo and Xiao 2003), friction problems and other research fields, scientist pay close attention to the orthotropic problem for thermoelasticity, thermoplastic (Ozaki 2012), elastic-plastic and other constitutive models.

This paper develops RFEM for the plane orthotropic problem by using the complete polynomial solutions of the mechanics equations. The number of element nodes  $N$  and the number of interpolation functions  $k$  are introduced for general analysis. The stiffness matrix when  $2N=k$  and the condensation stiffness matrix when  $k>2N$  are given, and the specific matrixes for 4 and 5 nodes are derived. The patch test is taken into account for RFEM, and the numerical results demonstrate the superiority of RFEM.

## 2. The governing equations and their fundamental solutions

In this paper, the plane orthotropic problem is discussed. In the rectangular coordinate system  $xOy$ , the relationship between strains  $\varepsilon_x$ ,  $\varepsilon_y$  and  $\gamma_{xy}$  and stresses  $\sigma_x$ ,  $\sigma_y$  and  $\tau_{xy}$  can be described as

$$\begin{bmatrix} \varepsilon_x \\ \varepsilon_y \\ \gamma_{xy} \end{bmatrix} = \begin{bmatrix} D_{11} & D_{12} & 0 \\ D_{12} & D_{22} & 0 \\ 0 & 0 & D_{66} \end{bmatrix} \begin{bmatrix} \sigma_x \\ \sigma_y \\ \tau_{xy} \end{bmatrix} = \mathbf{D}\boldsymbol{\sigma} \quad (1)$$

or

$$\begin{bmatrix} \sigma_x \\ \sigma_y \\ \tau_{xy} \end{bmatrix} = \begin{bmatrix} C_{11} & C_{12} & 0 \\ C_{12} & C_{22} & 0 \\ 0 & 0 & C_{66} \end{bmatrix} \begin{bmatrix} \varepsilon_x \\ \varepsilon_y \\ \gamma_{xy} \end{bmatrix} \tag{2}$$

where  $D_{ij}(i,j=1,2,6)$  and  $D_{ij}(i,j=1,2,6)$  are the flexibility and stiffness coefficients, respectively. The compatibility equation between the strains and displacements  $u, v$  in the  $x, y$  directions are

$$\varepsilon_x = \frac{\partial u}{\partial x} \quad \varepsilon_y = \frac{\partial v}{\partial y} \quad \gamma_{xy} = \frac{\partial u}{\partial y} + \frac{\partial v}{\partial x} \tag{3}$$

The equilibrium equations among stresses without body force are

$$\frac{\partial \sigma_x}{\partial x} + \frac{\partial \tau_{xy}}{\partial y} = 0 \quad \frac{\partial \sigma_y}{\partial y} + \frac{\partial \tau_{xy}}{\partial x} = 0 \tag{4}$$

Substituting Eq. (2) and Eq. (3) into the above equations, the equilibrium equations expressed by the displacements can be obtain as

$$\begin{aligned} C_{11} \frac{\partial^2 u}{\partial x^2} + (C_{12} + C_{66}) \frac{\partial^2 v}{\partial x \partial y} + C_{66} \frac{\partial^2 u}{\partial y^2} &= 0 \\ C_{22} \frac{\partial^2 v}{\partial y^2} + (C_{12} + C_{66}) \frac{\partial^2 u}{\partial x \partial y} + C_{66} \frac{\partial^2 v}{\partial x^2} &= 0 \end{aligned} \tag{5}$$

Let displacements  $u$  and  $v$  be a set of  $n$ -order polynomial solutions

$$u = \sum_{i=0}^n \alpha_i^{(n)} x^{n-i} y^i \quad v = \sum_{i=0}^n \beta_i^{(n)} x^{n-i} y^i \tag{6}$$

where  $\alpha_i^{(n)}, \beta_i^{(n)}$  are undetermined coefficients and their number is  $2(n+1)$ . Substituting the above expressions into Eq. (5), the relationships for the coefficients  $\alpha_i^{(n)}, \beta_i^{(n)}$  can be obtained. Notice that in Eq. (6),  $u, v$  are  $n$ -order polynomials, and the number of equations describing  $\alpha_i^{(n)}, \beta_i^{(n)}$  should be  $2(n-1)$ . By arbitrarily choosing 4 coefficients to be an independent set, the other coefficients can be obtained. Of course, some solutions with definite physical meanings can be chosen as linearly independent solutions. Obviously, Eq. (5) is always valid when  $n \leq 1$  and always has 4 solutions when  $n \geq 2$ .

For example, when  $n=3$ , Eq. (6) can be written as

$$\begin{cases} u = \alpha_0^{(3)} x^3 + \alpha_1^{(3)} x^2 y + \alpha_2^{(3)} x y^2 + \alpha_3^{(3)} y^3 \\ v = \beta_0^{(3)} x^3 + \beta_1^{(3)} x^2 y + \beta_2^{(3)} x y^2 + \beta_3^{(3)} y^3 \end{cases} \tag{7}$$

Substituting this into Eq. (5) produces two linear equations with six unknowns

$$\begin{cases} \left[ 6C_{11}\alpha_0^{(3)} + 2C_{66}\alpha_2^{(3)} + 2(C_{12} + C_{66})\beta_1^{(3)} \right] x + \left[ 6C_{66}\alpha_3^{(3)} + 2C_{11}\alpha_1^{(3)} + 2(C_{12} + C_{66})\beta_2^{(3)} \right] y = 0 \\ \left[ 6C_{66}\beta_0^{(3)} + 2C_{22}\beta_2^{(3)} + 2(C_{12} + C_{66})\alpha_1^{(3)} \right] x + \left[ 6C_{22}\beta_3^{(3)} + 2C_{66}\beta_1^{(3)} + 2(C_{12} + C_{66})\alpha_2^{(3)} \right] y = 0 \end{cases} \tag{8}$$

Based on the arbitrariness of  $x, y$ , there are four equations for eight undetermined coefficients  $\alpha_0^{(3)} \sim \alpha_3^{(3)}, \beta_0^{(3)} \sim \beta_3^{(3)}$

$$\begin{cases} 6C_{11}\alpha_0^{(3)} + 2C_{66}\alpha_2^{(3)} + 2(C_{12} + C_{66})\beta_1^{(3)} = 0 \\ 6C_{66}\alpha_3^{(3)} + 2C_{11}\alpha_1^{(3)} + 2(C_{12} + C_{66})\beta_2^{(3)} = 0 \\ 6C_{66}\beta_0^{(3)} + 2C_{22}\beta_2^{(3)} + 2(C_{12} + C_{66})\alpha_1^{(3)} = 0 \\ 6C_{22}\beta_3^{(3)} + 2C_{66}\beta_1^{(3)} + 2(C_{12} + C_{66})\alpha_2^{(3)} = 0 \end{cases} \tag{9}$$

By choosing  $\{\alpha_0^{(3)}, \alpha_1^{(3)}, \beta_0^{(3)}, \beta_1^{(3)}\}$  as the independent set, solving the above equations, and then substituting the solutions into Eq. (7), the four linear independent solutions are

$$\begin{cases} u = C_{22}C_{66}x^3 - 3C_{11}C_{22}xy^2 \\ v = C_{11}(C_{12} + C_{66})y^3 \end{cases}$$

$$\begin{cases} u = C_{66}(C_{12} + C_{66})y^3 \\ v = C_{22}C_{66}x^3 - 3C_{66}^2xy^2 \end{cases}$$

$$\begin{cases} u = [(C_{12} + C_{66})^2 - C_{11}C_{22}]y^3 + 3C_{22}C_{66}x^2y \\ v = -3C_{66}(C_{12} + C_{66})xy^2 \end{cases}$$

$$\begin{cases} u = -3C_{22}(C_{12} + C_{66})xy^2 \\ v = (C_{12}^2 + 2C_{12}C_{66})y^3 + 3C_{22}C_{66}x^2y \end{cases} \tag{10}$$

When  $n=0, 1$  or  $2$ , the fundamental solutions of Eq. (5) are listed in Table 1. Obviously, there are 2 linearly independent solutions when  $n=0$ , which implies rigid body translation in the  $x,y$  directions. When  $n=1$ , there are 4 linearly independent solutions, which implies rigid body rotation and uniform tension along the  $x,y$  directions and constant shear force bending. When  $n=2$ , there are also 4 linearly independent solutions, which implies pure bending in the  $x,y$  directions and a combination of bending and torsion along the  $x,y$  directions.

Table 1 Fundamental solutions of plane orthotropic elasticity with  $n \leq 2$

$n$	$u$	$v$	$\sigma_x$	$\sigma_y$	$\tau_{xy}$
0	1	0	0	0	0
	0	1	0	0	0
1	$y$	$-x$	0	0	0
	$D_{11}x$	$D_{12}y$	1	0	0
	$D_{12}x$	$D_{22}y$	0	1	0
	$D_{66}y/2$	$D_{66}x/2$	0	0	1
2	$D_{11}xy$	$(-D_{11}x^2 + D_{12}y^2)/2$	$y$	0	0
	$(D_{12}x^2 - D_{22}y^2)/2$	$D_{22}xy$	0	$x$	0
	$D_{12}xy$	$[-(D_{12} + D_{66})x^2 + D_{22}y^2]/2$	0	$y$	$-x$
	$[D_{11}x^2 - (D_{12} + D_{66})y^2]/2$	$(D_{12}x^2 - D_{22}y^2)/2$	$x$	0	$-y$

The fundamental solutions of plane orthotropic elasticity when  $n \geq 3$  can be obtained in a similar manner. They are not listed because they do not appear in the equations in this paper.

### 3. The construction of the rational finite element

In the rational finite element method, the displacement field of the element is given by the following interpolation formulation

$$u = \sum_{i=1}^k a_i u_i, \quad v = \sum_{i=1}^k a_i v_i \tag{11}$$

where  $a_i$  are the generalized displacements,  $k$  is the number of interpolation functions, and  $u_i, v_i (i=1, 2, \dots, k)$  are the fundamental solutions when they are arranged in an ascending about order  $n$ .

Suppose the number of nodes of the constructing element is  $N/2$  and there are two independent degrees of freedom of displacement on each node, that is, the total number of independent degrees of freedom in the element is  $N$ .

First,  $k$  should satisfy  $k \geq N$ . Second, in view of the completeness of the solution, all fundamental solutions for the proper  $n$ -order polynomial should be used completely. For example,  $k$  should be 6 ( $n \leq 1$ ), 10 ( $n \leq 2$ ), etc.

According to Eq. (11), the stress field of the element is given by

$$\sigma_x = \sum_{i=1}^k a_i \sigma_{xi}, \quad \sigma_y = \sum_{i=1}^k a_i \sigma_{yi}, \quad \tau_{xy} = \sum_{i=1}^k a_i \tau_{xyi} \tag{12}$$

Therefore, the energy of deformation of an element occupying region  $\Omega$  can be obtained as

$$U_e = \frac{1}{2} \iint_{\Omega} \boldsymbol{\sigma}^T \mathbf{D} \boldsymbol{\sigma} dx dy = \frac{1}{2} \mathbf{a}^T \mathbf{R} \mathbf{a} \tag{13}$$

where

$$\mathbf{a} = \{a_1, a_2, a_3, \dots, a_k\}^T \tag{14}$$

and  $\mathbf{R}$  is the generalized stiffness matrix between the generalized displacement  $\mathbf{a}$  and the generalized force  $\mathbf{g}$

$$\mathbf{g} = \mathbf{R} \mathbf{a} \tag{15}$$

For example, when  $k=10$ , the generalized stiffness matrix  $\mathbf{R}$  is

$$\mathbf{R} = \begin{bmatrix} \mathbf{0}_{3 \times 3} & \mathbf{0}_{3 \times 3} & \mathbf{0}_{3 \times 4} \\ \mathbf{0}_{3 \times 3} & \mathbf{R}_{11} & \mathbf{R}_{12} \\ \mathbf{0}_{4 \times 3} & \mathbf{R}_{12}^T & \mathbf{R}_{22} \end{bmatrix} \tag{16}$$

where

$$\mathbf{R}_{11} = \begin{bmatrix} D_{11}A & D_{12}A & 0 \\ D_{12}A & D_{22}A & 0 \\ 0 & 0 & D_{66}A \end{bmatrix} = \mathbf{D} \mathbf{A}$$

$$\mathbf{R}_{12} = \begin{bmatrix} D_{11}Q_x & D_{12}Q_x & D_{11}Q_y & D_{12}Q_y \\ D_{12}Q_x & D_{22}Q_x & D_{12}Q_y & D_{22}Q_y \\ 0 & -D_{66}Q_y & -D_{66}Q_x & 0 \end{bmatrix}$$

$$\mathbf{R}_{22} = \begin{bmatrix} D_{11}I_x & D_{12}I_x & D_{11}I_{xy} & D_{12}I_{xy} \\ D_{12}I_x & D_{22}I_x + D_{66}I_y & (D_{12} + D_{66})I_{xy} & D_{22}I_{xy} \\ D_{11}I_{xy} & (D_{12} + D_{66})I_{xy} & D_{66}I_x + D_{11}I_y & D_{12}I_y \\ D_{12}I_{xy} & D_{22}I_{xy} & D_{12}I_y & D_{22}I_y \end{bmatrix} \quad (17)$$

In the above expressions,  $A$  is the area of the element, and  $Q_x$ ,  $Q_y$ ,  $I_x$ ,  $I_y$ ,  $I_{xy}$  are first-order and second-order moments about the coordinate axes  $x, y$

$$A = \iint_{\Omega} dx dy, \quad Q_x = \iint_{\Omega} x dx dy, \quad Q_y = \iint_{\Omega} y dx dy$$

$$I_x = \iint_{\Omega} y^2 dx dy, \quad I_y = \iint_{\Omega} x^2 dx dy, \quad I_{xy} = \iint_{\Omega} xy dx dy \quad (18)$$

Obviously,  $\mathbf{R}_{11}$  corresponds to the linear displacement mode, while  $\mathbf{R}_{22}$  corresponds to the quadratic displacement mode. If the origin of the local coordinates is chosen to be in the center of the element,  $Q_x$ ,  $Q_y$  in  $\mathbf{R}_{11}$  vanish.

Because  $\mathbf{R}$  is the generalized stiffness matrix for the generalized displacement  $\mathbf{a}$  for which the global stiffness matrix of the structure is assembled from the element stiffness matrices according to the node displacement, the element stiffness matrix  $\mathbf{K}$ , which corresponds to the node displacement of element  $\mathbf{d}$ , must be given, i.e.

$$U_e = \frac{1}{2} \mathbf{d}^T \mathbf{K} \mathbf{d} \quad (19)$$

Substituting the coordinate of the nodes into Eq. (11) gives the transformation matrix  $\mathbf{T}$  between the generalized displacement  $\mathbf{a}$  and the node displacement  $\mathbf{d}$

$$\mathbf{d} = \mathbf{T} \mathbf{a} \quad (20)$$

The column form of the matrix is

$$\mathbf{T} = [\boldsymbol{\varphi}_1 \quad \boldsymbol{\varphi}_2 \quad \cdots \quad \boldsymbol{\varphi}_{k-1} \quad \boldsymbol{\varphi}_k] \quad (21)$$

The dimension of the column vector  $\boldsymbol{\varphi}_i (i=1 \sim k)$  is  $N$ .

When  $k=N$ , in general, the transformation matrix  $\mathbf{T}$  is an invertible square matrix; when  $k>N$ , the matrix  $\mathbf{T}$  is invertible. This will be discussed based on the relationship between  $N$  and  $k$ .

### 3.1 The case of $N=k$

Substitute Eq. (20) into Eq. (19) gives the energy of deformation of the element

$$U_e = \frac{1}{2} \mathbf{d}^T \mathbf{K} \mathbf{d} \quad (22)$$

where

$$\mathbf{K} = \mathbf{T}^{-\text{T}} \mathbf{R} \mathbf{T}^{-1} \quad (23)$$

is the stiffness matrix. The node force  $\mathbf{f}$  can be given as

$$\mathbf{f} = \mathbf{K} \mathbf{d} \quad (24)$$

and the relationship between the generalized force  $\mathbf{g}$  and the node force  $\mathbf{f}$  is

$$\mathbf{f} = \mathbf{T}^{-\text{T}} \mathbf{g} \quad (25)$$

In general, the current stiffness matrix  $\mathbf{K}$  cannot pass the patch test because the continuity of displacement and stress is destroyed in the boundary of the element. The matrix should be modified.

Research has been conducted on an element patch that has at least one inner node. When the boundary nodes of the patch are imposed on the displacement corresponding to a uniform stress field, solving the global stiffness matrix equations gives the displacement of inner node(s). If the displacement of the inner nodes agrees with the uniform stress field, the element passes the patch test.

This paper uses the technique to test the element. The result shows why the matrix  $\mathbf{K}$  cannot pass the test and gives the modification of matrix.

The one-element test is requested firstly when the node displacement involves rigid body translation or rotation; the stress of the element is zero. The second request occurs when a simple stress field  $\boldsymbol{\sigma}$  is applied to the element. The generalized force vector  $\mathbf{g}^{(s)}$  and the generalized force vector  $\mathbf{g}^{(t)}$ , which corresponds to the exact displacement field, should be equal. The superscript  $(s)$  means simple, and the superscript  $(t)$  means theory.

For the first request, if the node displacements are rigid displacements, according to the displacement interpolation formulation in Eq. (11),  $a_i \neq 0 (i=1 \sim 3)$  and  $a_j = 0 (j=4 \sim k)$ . Therefore, the stress interpolation formulation in Eq. (12) is zero. That is to say, the matrix satisfies the first request of the patch test.

In the second request, the so-called simple stress field refers to the element that has only the stress  $\sigma_x=1$  or  $\sigma_y=1$  or  $\tau_{xy}=1$ . Take the element with just the simple stress field  $\boldsymbol{\sigma}_x^{(s)} = \{1 \ 0 \ 0\}^{\text{T}}$  as an example. This field corresponds to the following generalized displacement vector

$$\mathbf{a}_{\sigma_x} = [0 \ 0 \ 0 \ 1 \ 0 \ \dots \ 0]^{\text{T}} \quad (26)$$

The forth element of vector  $\mathbf{a}$  is 1, and the others are 0.

The generalized force vector corresponding to the exact displacement vector is

$$\mathbf{g}_x^{(s)} = \mathbf{R} \mathbf{a}_x^{(s)} = [0 \ 0 \ 0 \ D_{11}A \ D_{12}A \ 0 \ 0 \ 0 \ 0 \ 0 \ h_{11,x} \ \dots \ h_{k,x}]^{\text{T}} \quad (27)$$

where  $h_{i,x} (i=11 \sim k)$  are nonzero coefficients and  $h_{i,x}=0 (i=7 \sim 10)$ .

Because the boundary of the element is linear while the stress is uniform, the boundary force can contribute to the element node. The lumped node force vector is noted as  $\mathbf{f}_x^{(t)}$ . The form of node force  $\mathbf{f}_x^{(t)}$  depends on the distribution of the nodes. Therefore, the generalized force vectors corresponding to the exact displacement are

$$\mathbf{g}_x^{(t)} = \mathbf{T}^{\text{T}} \mathbf{f}_x^{(t)} = [\boldsymbol{\varphi}_1^{\text{T}} \mathbf{f}_x^{(t)} \quad \boldsymbol{\varphi}_2^{\text{T}} \mathbf{f}_x^{(t)} \quad \dots \quad \boldsymbol{\varphi}_{k-1}^{\text{T}} \mathbf{f}_x^{(t)} \quad \boldsymbol{\varphi}_k^{\text{T}} \mathbf{f}_x^{(t)}]^{\text{T}} \quad (28)$$

Notice that  $\boldsymbol{\varphi}_1, \boldsymbol{\varphi}_2, \boldsymbol{\varphi}_3$  are derived from the rigid body displacements, so

$$\boldsymbol{\varphi}_i^T \mathbf{f}_x^{(t)} = 0 \quad (i = 1, 2, 3) \tag{29}$$

In addition,  $\boldsymbol{\varphi}_4, \boldsymbol{\varphi}_5, \boldsymbol{\varphi}_6$  are derived from the linear displacements, so

$$\boldsymbol{\varphi}_4^T \mathbf{f}_x^{(t)} = D_{11}A \quad \boldsymbol{\varphi}_5^T \mathbf{f}_x^{(t)} = D_{12}A \quad \boldsymbol{\varphi}_6^T \mathbf{f}_x^{(t)} = 0 \tag{30}$$

Eq. (28) can be rewritten as

$$\mathbf{g}_x^{(t)} = \mathbf{T}^T \mathbf{f}_x^{(t)} = [0 \quad 0 \quad 0 \quad D_{11}A \quad D_{12}A \quad 0 \quad \boldsymbol{\varphi}_7^T \mathbf{f}_x^{(t)} \quad \cdots \quad \boldsymbol{\varphi}_k^T \mathbf{f}_x^{(t)}]^T \tag{28}'$$

Compare  $\mathbf{g}_x^{(t)}$  in the above equation and  $\mathbf{g}_x^{(s)}$  in Eq. (27): the transformation matrix  $\mathbf{T}$  cannot ensure that the corresponding stiffness matrix will pass the test.

Of course, the other two simple stress fields have similar formulations. For only  $y$ -direction tension

$$\mathbf{g}_y^{(s)} = \mathbf{R} \mathbf{a}_y^{(s)} = [0 \quad 0 \quad 0 \quad D_{12}A \quad D_{22}A \quad 0 \quad 0 \quad 0 \quad 0 \quad 0 \quad h_{11,y} \quad \cdots \quad h_{k,y}]^T \tag{31}$$

$$\mathbf{g}_y^{(t)} = \mathbf{T}^T \mathbf{f}_y^{(t)} = [0 \quad 0 \quad 0 \quad D_{12}A \quad D_{22}A \quad 0 \quad \boldsymbol{\varphi}_7^T \mathbf{f}_y^{(t)} \quad \cdots \quad \boldsymbol{\varphi}_k^T \mathbf{f}_y^{(t)}]^T \tag{32}$$

where  $h_{i,y}(i=11 \sim k)$  are nonzero coefficients and  $h_{i,y}=0(i=7 \sim 10)$ .  $\mathbf{f}_y^{(t)}$  is the exact node force. For only shear stress is applied to the element

$$\mathbf{g}_{xy}^{(s)} = \mathbf{R} \mathbf{a}_{xy}^{(s)} = [0 \quad 0 \quad 0 \quad 0 \quad 0 \quad D_{66}A \quad 0 \quad 0 \quad 0 \quad 0 \quad h_{11,xy} \quad \cdots \quad h_{k,xy}]^T \tag{33}$$

$$\mathbf{g}_{xy}^{(t)} = \mathbf{T}^T \mathbf{f}_{xy}^{(t)} = [0 \quad 0 \quad 0 \quad 0 \quad 0 \quad D_{66}A \quad \boldsymbol{\varphi}_7^T \mathbf{f}_{xy}^{(t)} \quad \cdots \quad \boldsymbol{\varphi}_k^T \mathbf{f}_{xy}^{(t)}]^T \tag{34}$$

where  $h_{i,xy}(i=11 \sim k)$  are nonzero coefficients and  $h_{i,xy}=0(i=7 \sim 10)$ .  $\mathbf{f}_{xy}^{(t)}$  is the exact node force.

Modify the 7<sup>th</sup> to  $k^{\text{th}}$  column of matrix  $\mathbf{T}$ . Let

$$\tilde{\boldsymbol{\varphi}}_i = \boldsymbol{\varphi}_i + \eta_1^{(i)} \boldsymbol{\varphi}_4 + \eta_2^{(i)} \boldsymbol{\varphi}_5 + \eta_3^{(i)} \boldsymbol{\varphi}_6 \tag{35}$$

where  $\eta_j^{(i)}(j=1 \sim 3)$  are undetermined parameters. Respectively, transpose  $\mathbf{f}_x^{(t)}, \mathbf{f}_y^{(t)}, \mathbf{f}_{xy}^{(t)}$ , multiply with the above equation, and compare with Eq. (27), Eq. (31) and Eq. (33)

$$A \begin{bmatrix} D_{11} & D_{12} & 0 \\ D_{12} & D_{22} & 0 \\ 0 & 0 & D_{66} \end{bmatrix} \begin{bmatrix} \eta_1^{(i)} \\ \eta_2^{(i)} \\ \eta_3^{(i)} \end{bmatrix} = \begin{bmatrix} -\mathbf{f}_x^{(t)T} \boldsymbol{\varphi}_i + h_{i,x} \\ -\mathbf{f}_y^{(t)T} \boldsymbol{\varphi}_i + h_{i,y} \\ -\mathbf{f}_{xy}^{(t)T} \boldsymbol{\varphi}_i + h_{i,xy} \end{bmatrix} \tag{36}$$

Solve for  $\eta_j^{(i)}(j=1 \sim 3)$  and substitute them into Eq. (35). This new  $\tilde{\boldsymbol{\varphi}}_i(i = 7 \sim k)$  should replace the column vector  $\boldsymbol{\varphi}_i(i = 7 \sim k)$  of matrix  $\mathbf{T}$ . Note the modified transformation matrix as

$$\tilde{\mathbf{T}} = [\boldsymbol{\varphi}_1 \quad \boldsymbol{\varphi}_2 \quad \boldsymbol{\varphi}_3 \quad \boldsymbol{\varphi}_4 \quad \boldsymbol{\varphi}_5 \quad \boldsymbol{\varphi}_6 \quad \tilde{\boldsymbol{\varphi}}_7 \quad \cdots \quad \tilde{\boldsymbol{\varphi}}_k] \tag{37}$$

The corresponding modified stiffness matrix is

$$\tilde{\mathbf{K}} = \tilde{\mathbf{T}}^{-T} \mathbf{R} \tilde{\mathbf{T}}^{-1} \tag{38}$$

This is the stiffness matrix of the  $N$  node element. It passes the patch test.

### 3.2 The case of $N < k$

When the number of node degrees of freedom of the constructing element is less than the number of interpolation functions, the transpose matrix  $\mathbf{T}$  is a rectangular matrix that does not have an inverse matrix. So Therefore, Eq. (23) is a failure.

The first and simplest approach uses fewer fundamental solutions. Deleting arbitrary  $m=k-N$  rows of matrix  $\mathbf{T}$  gives a new transformation matrix  $\mathbf{T}'$ , which is a square matrix. The modification process described in the previous section could be applied. The corresponding stiffness matrix that can pass the patch test is

$$\tilde{\mathbf{K}}' = \tilde{\mathbf{T}}'^{-T} \mathbf{R}' \tilde{\mathbf{T}}'^{-1} \quad (39)$$

where  $\mathbf{R}'$  is a deleted square matrix.

This will lead to a poor result because the completeness of the solution is lacking. The solution will be directionally correlated and could even be wrong.

The second approach involves adding extra nodes and applying inner condensation in the element. By adding  $m/2$  nodes to the element, the number of node degrees of freedom of the augmented element is  $m+N=k$ . Applying the modification process described in the previous section to the augmented element yields the modified stiffness matrix  $\tilde{\mathbf{K}}$  and the transformation matrix  $\tilde{\mathbf{T}}$ . They are both  $k \times k$  square matrices.

Let the node displacement vector of the augmented element be

$$\mathbf{d} = \begin{bmatrix} \mathbf{d}_N \\ \mathbf{d}_m \end{bmatrix} \quad (40)$$

where  $\mathbf{d}_N$  is the node displacement of the constructing element and  $\mathbf{d}_m$  is the augmented node displacement.

Divide the stiffness matrix of the augmented element in the same way

$$\tilde{\mathbf{K}} = \begin{bmatrix} \tilde{\mathbf{K}}_{N,N} & \tilde{\mathbf{K}}_{N,m} \\ \tilde{\mathbf{K}}_{m,N} & \tilde{\mathbf{K}}_{m,m} \end{bmatrix} \quad (41)$$

The stress energy of this element is

$$U_e = \frac{1}{2} \mathbf{d}^T \tilde{\mathbf{K}} \mathbf{d} = \frac{1}{2} \begin{bmatrix} \mathbf{d}_N \\ \mathbf{d}_m \end{bmatrix}^T \begin{bmatrix} \tilde{\mathbf{K}}_{N,N} & \tilde{\mathbf{K}}_{N,m} \\ \tilde{\mathbf{K}}_{m,N} & \tilde{\mathbf{K}}_{m,m} \end{bmatrix} \begin{bmatrix} \mathbf{d}_N \\ \mathbf{d}_m \end{bmatrix} \quad (42)$$

Minimizing  $U_e$  yields

$$\mathbf{d}_m = \tilde{\mathbf{K}}_{m,m}^{-1} \tilde{\mathbf{K}}_{m,N} \mathbf{d}_N \quad (43)$$

Substituting the above equation into Eq. (42) yields

$$U_e = \frac{1}{2} \mathbf{d}_N^T \bar{\mathbf{K}} \mathbf{d}_N \quad (44)$$

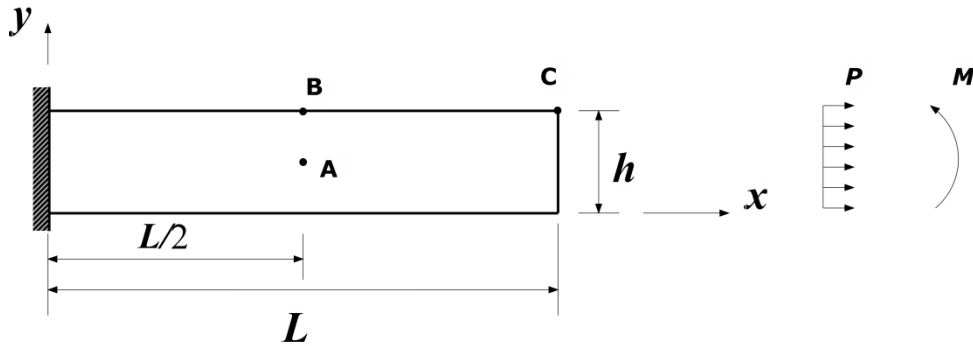


Fig. 1 The model of Example 1

Table 2 Results of Example 1

	Tension				Pure bending			
	$EPL/h$				$12EPL/h^2$		$12EML^2/h^3$	
$m*n$	$u_A$	$v_A$	$u_B$	$v_B$	$u_A$	$v_A$	$u_B$	$v_B$
2*4	0.489	0.501	0.000	0.016	0.000	0.249	-0.103	-0.101
4*4	0.495	0.500	0.000	0.015	0.000	0.250	-0.101	-0.101
Exact Solution	0.5	0.5	0	0.015	0	0.25	-0.1	-0.1

where

$$\bar{\mathbf{K}} = \tilde{\mathbf{K}}_{N,N} - \tilde{\mathbf{K}}_{N,m} \tilde{\mathbf{K}}_{m,m}^{-1} \tilde{\mathbf{K}}_{m,N} \tag{45}$$

which is just the stiffness matrix of the constructing element. There are  $N$  degrees of freedom.

#### 4. Numerical examples

The following examples only use the orthotropic rational quadrilateral element with 10 interpolation functions, i.e.,  $k=10$ . Hence two different elements are used. The 5-node element is named ORQ5T, and the corresponding condensation element is ORQ4T, where T means the element passes the patch test. The usual quadrilateral isoparametric element with 4 nodes is denoted as Q4.

**Example 1** The rectangular plate shown in Fig. 1 is considered. The length  $L$  is much larger than the width  $h$ . The left boundary is clamped, and the other boundaries are free. The flexibility coefficients are  $D_{11}=1/E$ ,  $D_{12}=-0.3/E$ ,  $D_{22}=3/E$  and  $D_{66}=5/E$ . Both the uniaxial tension  $P$  and the pure bending  $M$  are considered.

Two different FEM meshes are used for this example. For the first type of mesh, the  $x$  and  $y$  axes are divided equally into  $n$  and  $m$  intervals, respectively, so the meshes are all rectangular. The numerical results for different values of  $n$  and  $m$  and the exact solutions are given in Table 2, which shows the validity of the present method. The second mesh is shown in Fig. 2, and only pure bending is considered. As shown in Fig. 2, different values of  $e$  and  $d$  give different meshes, and point B is always the element node. The relative error is defined as

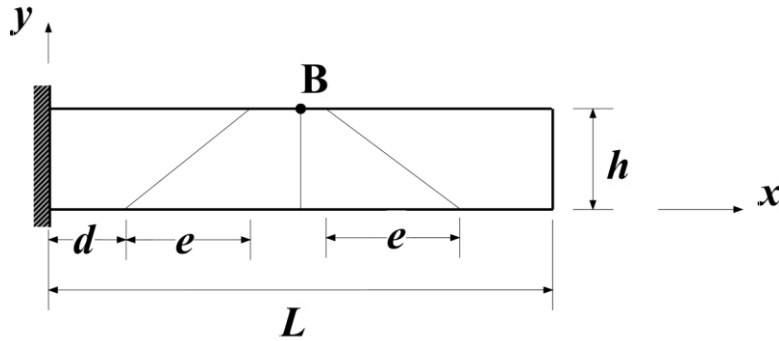


Fig. 2 The model of the sensitivity analysis

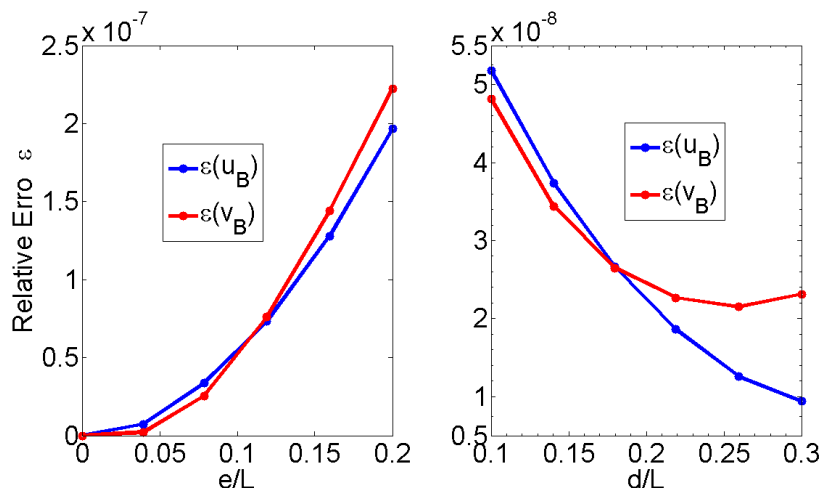


Fig. 3 Sensitivity analysis

$$\varepsilon = \|(u - \bar{u}) / \bar{u}\| \tag{46}$$

where  $u$  is the numerical result obtained using the proposed method and  $\bar{u}$  is the elastic theory solution. The relative error of point B for different values of  $e$  and  $d$  is given in Fig. 3, which shows that the method proposed in this paper has a better computational stability for a distorted mesh.

**Example 2** A square rule with  $l_1=h_1=10$ ,  $l_2=8$ ,  $h_2=2$  and  $h_3=8$  is shown in Fig. 4, in which C is the middle point of the end. The flexibility coefficients are the same as those given in Example 1, and a uniform downward load is applied to the end of the square rule. The domain is divided into 13 elements with 22 nodes (see Fig. 5), and ORQ4T, ORQ5T and Q4 are used to compute the displacement of A, B and C. A reference solution is also given by using Ansys, and the FEM mesh is shown in Fig. 6; the domain is divided into 1270 4-node plane elements. The relative errors for the displacement of points A, B and C are given in Table 3, in which the third, fourth, and fifth rows give the relative error obtained using ORQ4T, ORQ5T and Q4, respectively. The numerical results show that the algorithm proposed in this paper gives better results than the classic FEM for distorted elements.

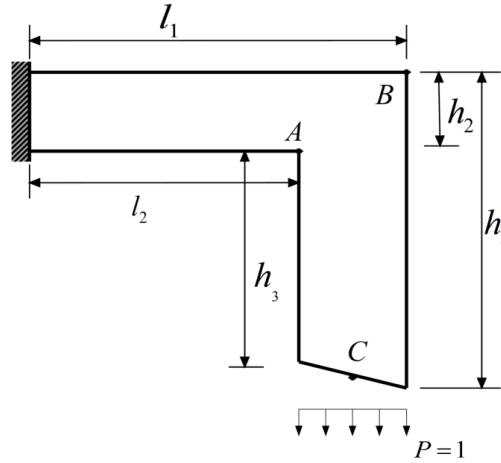


Fig. 4 The model of Example 2

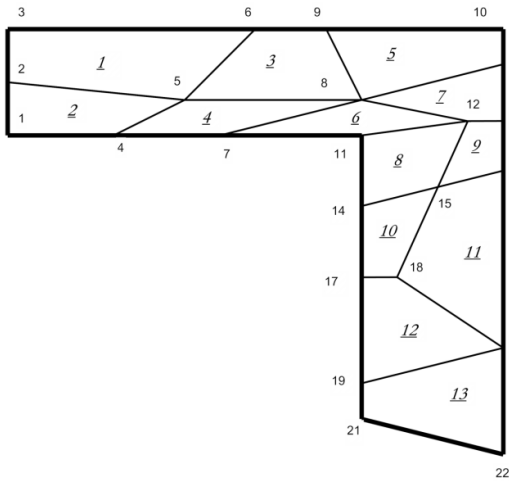


Fig. 5 The mesh for the proposed method in Example 2

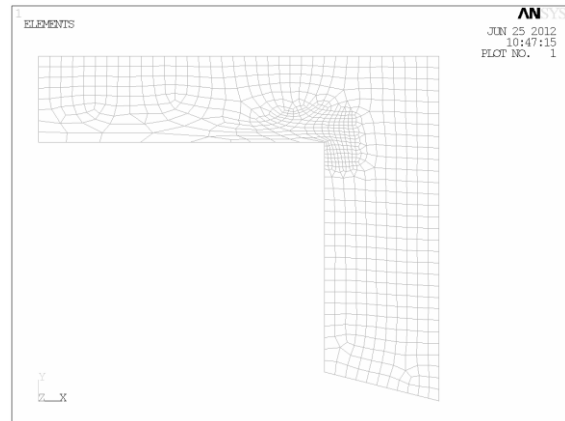


Fig. 6 The mesh for Ansys in Example 2

Table 3 The relative error of Example 2

	A		B		C	
	$u_A$	$v_A$	$u_B$	$v_B$	$u_C$	$v_C$
ORQ4T	6.814%	0.9792%	0.9012%	0.9167%	1.197%	0.8753%
ORQ5T	5.533%	0.8903%	0.9127%	0.8053%	1.216%	0.8146%
Q4	11.82%	18.20%	19.83%	15.39%	14.38%	12.57%
Ansys	-0.6554	-3.436	0.6619	-4.768	-5.673	-4.4146

**Example 3** Cook beam is a skew cantilever under shear distributes force at the free edge, shown as Fig. 7. The thickness of the beam is 1.0, the material is isotropic and the Young's module and Poison ratio are  $E=1.0$  and  $\mu=1/3$ . Compute this beam by  $2 \times 2$ ,  $4 \times 4$  and  $8 \times 8$  meshes with CQ4,

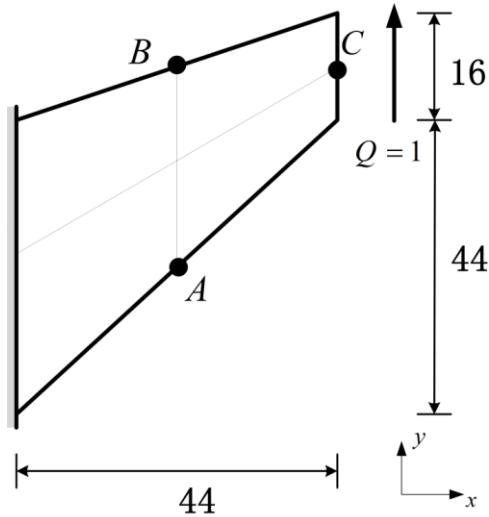


Fig. 7 The model of Example 3

Table 4 The result of Example 3

Element type	$v_C$			$\sigma_{Amax}$			$\sigma_{Amin}$		
	2×2	4×4	8×8	2×2	4×4	8×8	2×2	4×4	8×8
CQ4	11.80	18.29	22.08	0.1217	0.1873	0.2242	-0.0960	-0.1524	-0.1869
QAC-ATF4	24.36	23.84	23.89	0.2127	0.2277	0.2350	-0.1809	-0.1934	-0.2001
ORQT4	23.21	23.77	23.88	0.2059	0.2284	0.2333	-0.1893	-0.1948	-0.1999
CQ5	12.24	18.86	22.33	0.1039	0.1884	0.2253	-0.0551	-0.1410	-0.1858
QAC-ATF5	23.06	23.83	23.94	0.2074	0.2101	0.2284	-0.1832	-0.1974	-0.2025
ORQT5	23.31	23.80	23.94	0.2105	0.2311	0.2341	-0.1895	-0.1959	-0.2008
Reference solution		23.96			0.2362			-0.2023	

CQ5, QAC-ATF4 (Cen *et al.* 2009), QAC-ATF5 (Cen *et al.* 2009), ORQT4 and ORQT5. The results of CQ4, CQ5, QAC-ATF4 and QAC-ATF5 are all provided by Cen *et al.* (2009). The reference solution is provided by Long and Xu (1994) using element GT9M8 with 64×64 mesh. Table 3 gives the deflection at the middle point C of the free edge, the maximum principal stress at the middle point A of the lower edge, and the minimum principal stress at the middle point B of the upper edge. Table 3 shows that ORQT4 and ORQT5 gradually approach the reference solution when the meshes refined and so exhibit quite good convergence, that the deflection and stress of ORQT4 and ORQT5 are all quite better than conventional elements CQ4 and CQ5, and that the elements proposed in this paper have almost the same accuracy with QAC-ATF4 and QAC-ATF5.

#### 4. Conclusions

Different from standard FEM, RFEM is formulated in the physical domain using the analytical solutions of elastic problems. In this framework, for different materials and element

characteristics, the interpolation functions can change automatically. Numerical examples demonstrate that compared with standard FEM, RFEM produces more reliable numerical results, and the efficiency and stability of the present method are better. For distorted elements, the method produces more stable results. The method is valuable for the extension of RFEM to plane or 3D general anisotropy problems.

## References

- Areias, P.M.A. and Belytschko, T. (2005), "Analysis of three-dimensional crack initiation and propagation using extended finite element method", *Int. J. Numer. Meth. Eng.*, **63**(8), 760-788.
- Bambill, D.V., Rossit, C.A. and Susca, A. (2009), "Numerical experiments on the determination of stress concentration factors in orthotropic perforated plates subjected to in - plane loading", *Struct. Eng. Mech.*, **32**(4), 549-561.
- Beom, H.G., Cui, C.B. and Jang, H.S. (2012), "Application of an orthotropy rescaling method to edge cracks and kinked cracks in orthotropic two-dimensional solids", *Int. J. Eng. Sci.*, **51**, 14-31.
- Cen, S., Chen, X.M., Li, C.F. and Fu, X.R. (2009), "Quadrilateral membrane elements with analytical element stiffness matrices formulated by the new quadrilateral area coordinate method (QACM-II)", *Int. J. Numer. Meth. Eng.*, **77**(8), 1172-1200.
- Cen, S., Fu, X.R., Zhou, G.H., Zhou, M.J. and Li, C.F. (2011), "Shape-free finite element method: the plane hybrid stress-function (HS-F) element method for anisotropic materials", *Sci. China, Ser G*, **54**(4), 653-665.
- Cen, S., Zhou, G.H. and Fu, X.R. (2012), "A shape-free 8-node plane element unsymmetric analytical trial function method", *Int. J. Numer. Meth. Eng.*, **91**(2), 158-185.
- Duarte, C.A., Babuska, I. and Oden, J.T. (2000), "Generalized finite element methods for three dimensional structural mechanics problems", *Comput. Struct.*, **77**(2), 215-232.
- Fu, X.R., Cen, S., Li, C.F. and Chen, X.M. (2010), "Analytical trial function method for development of new 8-node plane element based on the variational principle containing Airy stress function", *Eng. Comput.*, **27**(4), 442-463.
- Hambli, R., Bettamer, A. and Allaoui, S. (2012), "Finite element prediction of proximal femur fracture pattern based on orthotropic behavior law coupled to quasi-brittle damage", *Med. Eng. Phys.*, **34**(2), 2-10.
- Ji, Z., Liu, Z.J. and Zhao, W. (2000), "8-Node curve quadrilateral rational finite element", *J. Dalian Univ. Technol.*, **40**(1), 40-44. (in Chinese)
- Ji, Z. and Zhong, W.X. (1997), "Rational plane quadrilateral four and five nodes finite elements", *Chin. J. Comput. Mech.*, **14**(1), 19-27. (in Chinese)
- Jirousek, J. and Venkatesh, A. (1992), "Hybrid trefftz plane elasticity elements with p-method capabilities", *Int. J. Numer. Meth. Eng.*, **35**(7), 1443-1472.
- Karihaloo, B.L. and Xiao, Q.Z. (2003), "Modeling of stationary and growing cracks in FE framework without remeshing: a state of the art review", *Comput. Struct.*, **81**(3), 119-129.
- Long, Y.Q. and Xu, Y. (1994), "Generalized conforming quadrilateral membrane element with vertex rigid rotational freedom", *Comput. Struct.*, **52**(4), 749-755.
- Long, Y.Q., Cen, S. and Long, Z.F. (2009), *Advanced Finite Element Method in Structural Engineering*, Springer-Verlag GmbH, Berlin Heidelberg, Germany, Tsinghua University Press, Beijing, China.
- Melenk, J.M. and Babuska, I. (1996), "The partition of unity method: basic theory and applications", *Comput. Meth. Appl. Mech. Eng.*, **139**(1), 289-314.
- Ozaki, S., Hikida, K. and Hashiguchi K. (2012), "Elastoplastic formulation for friction with orthotropic anisotropy and rotational hardening", *Int. J. Solid. Struct.*, **49**(3), 648-57.
- Simone, A., Duarte, C.A. and Van der Giessen, E. (2006), "A generalized finite element method for polycrystals with discontinuous grain boundaries", *Int. J. Numer. Meth. Eng.*, **67**(8), 1122-1145.
- Turner, M.J., Clough, R.W., Martin, H.C. and Topp, L.C. (1956), "Stiffness and deflections analysis of

- complex structures”, *J. Aeronaut. Sci.*, **23**(9), 805-809.
- Venkatesh, A. and Jirousek, J. (1995), “Accurate representation of local-effects due to concentrated and discontinuous loads in hybrid-trefftz plate-bending elements”, *Comput. Struct.*, **57**(5), 863-870.
- Wang, Y.F. and Zhong, W.X. (2002), “Plane 8-node rational finite element”, *Chin. J. Comput. Mech.*, **23**(1), 109-114. (in Chinese)
- Wang, Y.F. and Zhong, W.X. (2003), “A rational hexahedron 8-node finite element”, *Acta Mech. Sin.*, **20**(3), 131-135. (in Chinese)
- Xue, W.M., Karlovitz, L.A. and Atluri, S.N. (1985), “On the existence and stability conditions for mixed-hybrid finite element solutions based on Reissner’s variational principle”, *Int. J. Solid. Struct.*, **21**(1), 97-116.
- Zhong, W.X. (1997), “Convergence of FEM and the conditions of patch test”, *Chin. J. Comput. Mech.*, **14**(3), 251-262. (in Chinese)
- Zhong, W.X. and Ji, Z. (1996), “Rational finite element”, *Comput. Struct. Mech. Appl.*, **13**(1), 1-8. (in Chinese)
- Zhong, W.X. and Ji, Z. (1997), “The convergence proof of the plane rational finite element”, *Acta Mech. Sin.*, **29**(6), 676-685.